ABSTRACT

The treatment of corroded copper, brass and bronze ship fastenings often presents conservators with widely different responses from apparently similar or identical materials. This study demonstrates that the electrochemical techniques of measuring the polarization resistance and corrosion potentials of objects are powerful tools in resolving the differences in materials performance. The effects of sea water agitation, pH and dissolved oxygen on the above corrosion parameters are discussed. In the absence of any discernable differences in chemical composition, widely divergent corrosion rates can be rationalized in terms of the metal microstructure and the stresses induced at manufacture or during the shipwrecking process.

KEYWORDS
Composition, microstructure, copper, alloys, corrosivity, chloride.

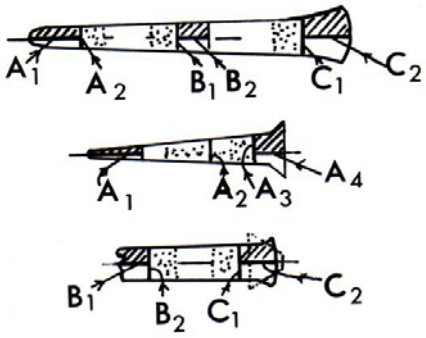

Fig. 1:Sectioning diagram for ships' fastenings

*Author to whom correspondence should be addressed

THE EFFECTS OF COMPOSITION AND MICROSTRUCTURE ON THE CORROSIVITY OF COPPER ALLOYS IN CHLORIDE MEDIA

Dr Ian Donald MacLeod* and Stephane Pennec
Western Australian Maritime Museum, Cliff Street, Fremantle, Western Australia, 6160, Australia

Introduction

Despite the plethora of papers that deal with corrosion of copper and its alloys in chloride media the research relates primarily to materials of high purity and well defined composition. [1,2,3] Conservators often find it difficult to bridge the gap between these model systems and the decaying artefact, which they have just been told to conserve. Objects recovered from both land and maritime archaeological sites often present the worst cases of corrosion and are the most difficult to stabilize. [4]

In an attempt to overcome this conundrum the Western Australian Museum has carried out corrosion and conservation research on artefacts recovered from the historic shipwrecks off our coast, which date back to the wreck of the *Trial* in 1622. The work of North and Pearson [5,6,7] is notable for the characterization of corrosion mechanisms of iron and for new treatments to conserve these highly degraded objects. More recently the on-site measurements of corrosion potentials and surface pH of corroding iron objects has provided details of corrosion mechanisms on the seabed and a potential method for dating archaeological iron.[8, 9] Similar studies on copper and its alloys have also been reported. [10,11]

A vast number of fastenings made of copper, brass and bronze have been recovered from the wrecks of the *Rapid* (1811), *James Matthews* (1841)[1, 2] and *Eglinton* (1852). A wide range of apparent long-term corrosion rates were observed on the artefacts during conservation treatment. Sometimes the materials were very similar in composition and yet they presented different problems. Many of the difficulties could be rationalized in terms of the micro-environment [13, 14] and the gross differences in site conditions – the *James Matthews* is anaerobic and buried under several metres of sand while the *Rapid* and *Eglinton* lie in shallow reef strewn waters at depths from 8 to 4 metres. This work is an extension of the previous studies which concentrated on the effects of microstructure on corrosion and on the industrial archaeology that could be revealed. [15,16]

This paper is an attempt to link traditional conservation techniques of metallographic and chemical analysis of artefacts which electrochemical parameters obtained on the same objects. Since impurities such as arsenic, antimony and bismuth commonly occur in copper and its alloys, a knowledge of the concentration and distribution in the parent metals can help explain the reasons why artefacts recovered from the same micro-environment will corrode at a different rate.[17]

This study reports on the effects of oxygenation on corrosion potentials (Ecorr) and the initial corrosion rates of ships fastenings in sea water. Electrochemistry when used in conjunction with metallography provides conservators with an invaluable tool in the search for new understanding.

Experimental

The nine spikes and nails were examined metallographically after they had been sectioned and embedded in Araldite D or in Bakelite. Surfaces were prepared by griding with wet and dry carborundum paper to 1200 grit and polishing with diamond past to ¼ micron; the etchant was 2 wt% ferric chloride in ethanol. Larger objects, up to 60cm long, sampled in six places with three longitudinal (LS) and three transverse sections (TS) representing the tail (shank), body and head regions of the fittings. Where the spikes had been broken in the shipwreck itself only four sections were taken since the tail of the fitting remained on site in the hull timbers.

Smaller objects such as nails, up to 15cm long, were sectioned in four ways; a longitudinal section at the tip, transverse sections in the middle of the body and under the head and a longitudinal section of the head. The sections are labelled according to the diagram illustrated in fig. 1.

Drilled core samples (360±100mg) were taken from each object and dissolved at room temperature in 10% nitric, 5% hydrochloric and 2% tartaric acids to avoid volatilisation of antimony. Core samples were taken in an attempt to overcome the problems associated with analysis of archaeological metals.[18] The alloys left no insoluble residues and the solutions were analysed using a Varian AA4 Spectrophotometer, except for arsenic which was determined commercially (ANALABS) by hydride generation. The results of the analyses are listed in Table I.

Vickers microhardness measurements on the polished sections were made using a Tukon Model 300 operating on a 400 gram load with a x10 objective; grain sizes were measured

with the same instrument or by the ASTM method using a metallurgical microscope. Several sections were examined under the scanning electron microscope at CSIRO Division of Mineralogy using the backscattered electron/low vacuum mode. Qualitative elemental analyses were done using the EDAX attached to the JSM2.

Electrical connections to the polished metal sections were effected by drilling through the plastic mounting resin and either soldering an insulated multi-strand copper cable to the rear of the section or by using electrically conducting epoxy resin. The cavity was then sealed with Araldite epoxy resin. The corrosion potentials were measured using a Metrohm calomel electrode (saturated with KC1) which was calibrated against a platinum electrode in a quinhydrone solution at pH 4.0. Voltages referred to in this paper are all relative to the saturated calomel electrode (SCE) unless otherwise stated. The water temperature was 22.5±1.5°C. Dissolved oxygen measurements were made using an ICI oxygen meter (411) after correction for the salinity of the sea water (35.5ppt). The sea water was filtered after collection from the ocean and was stored in a refrigerator when not in use. The current voltage curves for polarization resistance measurements were recorded using an AMEL 551 potentiostat with a platinum auxiliary electrode and an XY recorder – the current voltage data was collected over a range of ±2mV/sec. The effects of dissolved oxygen, stirring, etc. on Ecorr were determined using a Fluke 8010A digital multimeter. The measurements were made in a modified Metrohm polarographic cell which allowed side mounting of the metal sections.

Corrosion Potentials And Polarisation Resistance

When copper and its alloys are immersed in oxygenated sea water they will corrode at a rate that is dependent on their chemical composition, microstructure and on the amount of dissolved oxygen. [19,20] In aerated solutions the corrosion potential is the voltage of the corrosion cell consisting of the anodic (oxidation of metal) and cathodic (oxygen reduction) half cells. The corrosion rate at the corrosion potential is given by the corrosion current, i_{corr}, which is related to the polarisation resistance, Rp, via the expression

$$(\frac{\Delta E}{\Delta i})\Delta E \rightarrow 0 = R_p = B \diagup i_{corr}$$

The constant B can be calculated via Faraday's laws relating to weight loss data or it can be determined from analysis of electrochemical polarization data. In physical terms the value of B can be obtained from the Stern and Geary[21] relationship.

$$B = \frac{b_a b_c}{2.303(b_a + b_c)} = i_{corr} R_p$$

Were b_a and b_c are the anodic and cathodic decadic Tafel slopes. The value of B used to calculate the corrosion current is that previously determined from corrosion of *Rapid* bronze fittings in sea water.[22] Using the anodic Tafel slope b_a 46±2mV and the cathodic slope b_c of 56±3mV the value of B, using the formula above, is 11mV. Our calculated corrosion currents are based on measurements of R_p after 15-25 hours of exposure of the samples to sea water and as such they are approximately one order of magnitude too high[23] and should be regarded as initial corrosion rates, rather than average long-term values. Nevertheless, the corrosion currents provide a useful guide to the performance of the alloys.

Results and Discussion

The results of the polarisation resistance measurements on the mounted and polished sections are summarized in Table II. In order to facilitate comparisons the wet chemical analyses listed in Table I are shown in the same groupings. Since the R_p values are determined from the slopes of the current voltage curves as $(\Delta E/\Delta i)\Delta E \rightarrow O$ they are naturally dependent on the surface area exposed to the sea water so the i_{corr} values have been standardized to $\mu A.cm^{-2}$ (using the given surface areas) to enable the various R_p values to be properly compared.

Copper

The four spikes and nails appear to have essentially the same chemical composition since the differences in the analyses shown in Table I are only minor. However, when we look at the calculated i_{corr} vales we see that RP 3074 and JM 150/T13 are clearly corroding at a much higher rate than JM 150/T6 and JM 160/T8 and that the fittings clearly fall into two categories as far as corrosion currents are concerned. The only systematic chemical difference between the four fittings lies in their bismuth impurity concentrations with the lower corrosion rates corresponding with higher bismuth levels in the parent metal. In order to understand the causes for the 370% difference in corrosion rate between the two sets of copper fastenings we mush look at their microstructures.

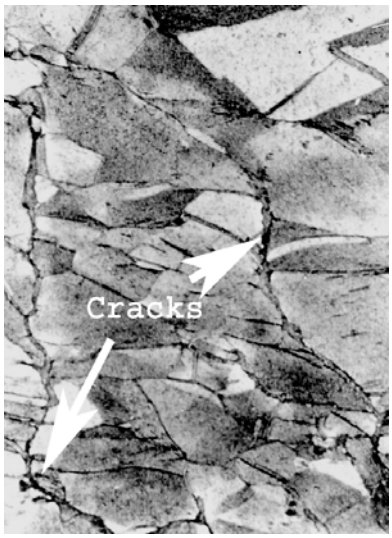

Fig. 2:Scanning electron micrograph of transcrystalline cracks and cold deformation of JM 150/T13 copper nail. Full width 110μm.

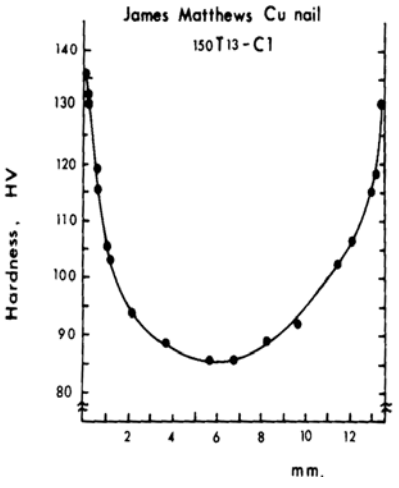

Fig. 3: Plot of the Vickers microhardness of the C1 transverse section of the JM 150/T13 copper nail

The C1 transverse section of RP 3074 was taken just below the head of the spike whose structure is described as being a leaded arsenical copper with small amounts of tin, antimony, silver and bismuth and traces of iron and zinc. The microstructure of the spike is formed with fully recrystallised grains of the primary solid solution α. Over the whole volume numerous Cu_2O and Pb-rich particles were found. Their shape and density of distribution depend on degree of deformation (the distortion is only seen in longitudinal sections since their shape is circular in transverse sections). There are more cuprite (Cu2O) inclusions than microdroplets of lead. The grains in the section are distorted as a result of cold-hammering of head. The hardness at the edge of the section had a value of 134 which fell to 120±2HV in the centre. By the way of contrast the middle of the shank, which is free of distortion, has a microhardness of 86HV.

The JM 150/T13 nail examined was also a transverse section below the head of the nail which is best described as an arsenical copper with a small amount (0.1wt%) of lead (see Table I). The microstructure is similar to RP 3074 but it also has some Cu_2S inclusions as well as the Cu_2O and Pb inclusions previously noted. The nail has clearly defined square had with bevelled edges and there are definite signs of transcrystalline cracks and cold deformation in the C1 section which was formed in the last stages of manufacture (see fig. 2). The hard working increases the hardness (HV) values from 86 for the fully recrystallised grains to a maximum value of 135. A typical plot of the way in which the hardness falls away with distance from the edge in shown in fig. 3. The higher corrosion rate of these two objects is probably a reflection of the stresses associated with the construction of the vessel (RP 3074) and the production of the nail itself (JM 150/T13). Increased corrosion rates as a result of surface strain and stress in coper has been the subject of intense study – annealing the metal causes a marked reduction in apparent corrosion rates. [24]

By way of comparison we can look at the microstructure of the other two fittings from the *James Matthews* which corrode at a much lower rate. The spike, JM 150/T6, has a composition very similar to both the JM 150/T13 and the *Rapid* spike except that it has higher tin (0.41%), arsenic (0.41%) and bismuth (0.128%) impurity levels. The spike when recovered from the wreck site was broken in the middle of the body (see fig. 1). The centre sections of the spike consist of fully recrystallised grains of α solid solution with a small number of Pb-rich as well as Cu_2O and Cu_2S inclusions. Since the microstructure is essentially uniform, the spike has either been annealed after being cold-worked or it has been hot-worked. The microhardness of the B2 transverse section (see fig. 1) from the middle of the shank had maximum values at the edge (HV values 110±2) which fell away to 86±3 in the centre. The absence of highly stressed and distorted grains combined with the high levels of arsenic impurities have apparently provided a good combination for corrosion resistance. Electron microprobe analysis has shown that impurities such as As, Sb, Bi, etc. tend to concentrate along the grain boundaries[25] where their effective concentration is increased and so small levels of these impurities can have a marked effect on the materials performance. The high level of bismuth does lead to transgranular cracking in the head[26] during extensive working but this section was not the subject of our electrochemical analysis.

The *James Matthews* nail 160/T8 has a composition which is essentially the same as 150/T6 and T13 except that it has a much higher bismuth impurity level (0.255%). The microstructure is significantly different in that it consists of deformed grains of the α solid solution with inclusions of Cu_2O, Cu_2S and Pb-rich materials. The deformation of grains and the presence of bent twins proves that shaping of the fitting took place by cold-hammering. The deformation is most noticeable in the sections close to the tip since by the time we reach the C1 transverse section under the head the microstructure was surprisingly uniform with typical hardness values of 112±4HV across its breadth. The higher hardness is due to the higher levels of bismuth and arsenic and is not a reflection of stress.[27] The differences in the corrosion performance of these four copper fittings can be seen as being due to a combination of the microstructure (the stress, hardness, etc. associated with the experiences of the artefact from the time of manufacture, through shipwreck to recovery) and the amount of trace impurities such as arsenic and bismuth. The high levels of bismuth in the *James Matthews* made many of the spikes and boils very tough but brittle and may have indirectly determined the fate of the vessel.

Brass

Only two fittings were available for comparison, owing principally to the dates of manufacture of the vessels since in the early nineteenth century the majority of the fastenings were copper. The principal chemical difference between the *Rapid* brass spike and the *Eglinton* nail is that EG 1379 has 4.22% more zinc and that the *Rapid* spike is more heavily leaded (see Table I). The higher corrosion rate of the *Eglinton* brass, 28.3μA.cm^{-2} compared with 16.2μA.cm^{-2}, is a little surprising since the increase of 16% in the amount of zinc has been translated into a 75% increase in corrosion. There are, however, very interesting differences in the metallurgical structures of the two samples, which help to explain the large increase.

The A_2 transverse section of RP 0000/T13 was made just under the head of the spike. The spike

has a high led content (1.9%) and a small amount of tin (0.41%) as an impurity. The microstructure is formed with cored dendrites of primary α solid solution and a tin-rich phase which is present in interdendritic regions. Pb-rich particles are placed in interdendritic regions as well, individually or in association with tin-rich phases and their shape is most angular and they sporadically fill shrinkage cavities. The structure and colour of the spike is typical of a 70/30 brass with a small amount of Sn. The microhardness is greater closer to the surface with 160±10HV values occurring in the first 2mm in association with the tin-rich interdendritic phase; the mean hardness of the α cored (copper-rich) dendrites is 132±4HV. Because lead is the last component to solidify in tends to minimize the ingress of sea water through casting defects and thereby enhances the corrosion performance of the alloy.

The *Eglinton* 1379/T2 nail is a medium leaded 70/30 brass with a small amount of tin (0.29%). Apart from the higher zinc content its composition is remarkably similar to the *Rapid* spike. The microstructure is typical of a cast α brass (cored dendrites of α solid solution) which contains a small amount of the zinc-rich β phase in the interdendritic areas. In these areas Pb-rich particles are also found. The presence of "hot tear" fractures is probably due to premature removal of the nail from the mould when the β phase had not fully solidified. It is possible that the tear lines were not as deep as they currently appear but that the initial defect has been exacerbated by 125 years of corrosion. The crack has undergone extensive dezincification of the zinc-rich β phase. The normally beneficial effect of arsenic on dezincification has probably been masked by the relatively high level of iron (0.165%) as an impurity.[28] Microhardness measurements showed that C1 section had values that varied from 182HV for the qui-axed grains (40x40μm) in the centre to 141Hvto the columnar grains (104x19μm) at the outer edge. The hardness varied in a linear fashion with increasing distance from the outer surface at the rate of 21 units per mm and is directly related to the grain shape and size. The higher corrosion rate of the *Eglinton* nail is directly related to the greater amount of zinc in the alloy since without the extra zinc there would have been insufficient β phase present to allow the "hot tear" to occur. The greater chemical reactivity of the zinc-rich β phase provides a greater driving force for interdendritic corrosion.

Bronze

The deliberate addition of tin to copper has long been known to enhance the corrosion resistance of the alloy. Analysis of the three bronze nails (Table I) shows that the corrosion rates apparently mimic the amount of tin in the alloy, namely the higher the amount of tin, the lower is the apparent corrosion rate in the fully oxygenated sea water test solutions. The differences in corrosion rates are not due to the direct proportionality of composition but are also dependent on the microstructure of the bronzes.

The composition of the *James Matthews* 610 nail is, to say the least, highly unusual for the 19th century alloy. Although coper accounts for 90.74% of the weight, the tin content is only 3.60%. Apart from being a medium leaded bronze it also contains 0.84% bismuth, 1.396% arsenic and 2.32% nickel! (see Table I). The 25mm nail has an as-cast structure with the macrostructure consisting of a columnar zone and a couple of equi-axed relatively big grains in the centre of the nail. The microstructure, however, is typical of bronze containing higher amounts of tin (more than 10%) and has cored dendrites of primary α solid solution and a lot of islands of α plus δ eutectoid, which are placed in interdendritic areas. Pb-rich particles occur sporadically in the interdendritic areas with inclusions of zinc and lead sulphides. A lot of shrinkage cavities have been found in the transverse A_2 section near the head and there is 'tin sweat' under all of the surface. It would appear that the presence of the nickel, arsenic and bismuth (a total of 4.55 wt%) has dramatically changed the microstructure from that expected on the basis of the 3.6% tin. The microhardness at the tin-rich edge of the nail has vales of 340! It is likely that the high bismuth, arsenic and nickel impurities came from a copper sulphide ore body that also contained minerals such as Parkerite ($Ni_3Bi_2S_2$) and Gersdorffite (NiAsS). Since silver sulphides are also found in association with these minerals it is not surprising that JM 610 has the highest silver content, 0.235 wt%, of the fifty copper alloys analysed in these laboratories. The presence of Cu_2S inclusions in the *James Matthews* copper fittings supports the use of a copper sulphide ore body as the source of the metal in France. The shrinkage in the alloy effectively increases the read surface area of the metal, thereby enhancing the corrosion rate.

The high leaded zinc bronze nail RP 3373B with 4.8 wt% zinc has a typical cast structure based on cored dendrites of the primary α solid solution. Given its higher tin content (5.53 wt%) it is not surprising to find many more light coloured islands of the α plus δ eutectoid (circular or angular in shape) than in the JM610 bronze. There is rough gas porosity and shrinkage porosity over the transverse surface of the A_2 section (under the head of the nail) and this resulted from imperfect casting technology and would promote corrosion. There is a large area in the centre of the section with equi-axed grains. Tin-rich areas have been found in the interdendritic regions and there is also 'tin sweat' which results in a higher concentration of tin closer to the surface. The microhardness of the tin-rich areas was 178±6HV while the nickel-bismuth-arsenical bronze JM 610 had values as high as 340! In the middle of the section the hardness values were 120±5HV.

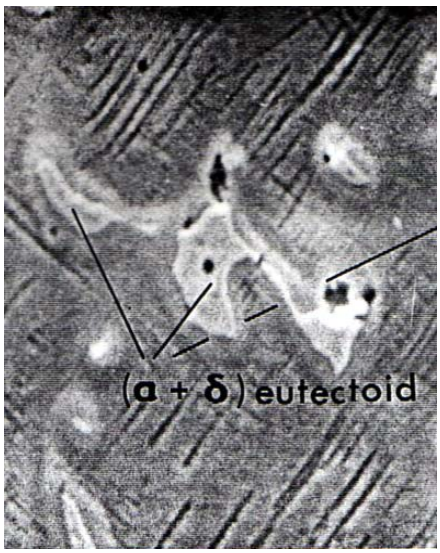

Fig. 4 Scanning electron micrograph of the RP 5004 bronze nail showing (light grey) islands of the α and δ eutectoid. Full width 190µm

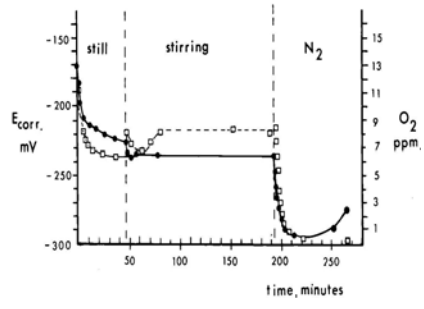

Fig. 5 Plot of the corrosion potential (mV vs SCE) and dissolved oxygen levels for the brass nail EG 1379/T2 in sea water as a function of time and water movement.

• = Ecorr, □ = dissolved oxygen.

The leaded bronze nail RP 5004 had a tin content of 7.46 wt% and was essentially free of zinc (see Table I). The nail exists in its as-cast state and has not been mechanically worked or heat treated and it has a characteristic dendritic cast structure. The microstructure is very similar to RP 3373B with cored dendrites of α solid solution and particles of α plus δ eutectoid (see fig. 4). Lead-rich particles and sulphide inclusions occur sporadically in interdendritic areas. A lot of shrinkage and gas porosity have been found in the volume of the nail, which is proof again of imperfect foundry practice. Under the whole surface there are large amounts of tin-rich areas which were formed as a result of 'tin sweat'. Microhardness values of 184±4HV were found in the 'tin sweat' areas and the mean value of 138±7HV for the transverse sections is higher than that observed for the lower tin content of RP 3373B. The main effect of the greater tin content is to increase the "hard" zone around the edges from 22µm (RP3373B) up to 1400µm in places.

Since there is no evidence of mechanical working in the three bronze nails there are no differences in corrosion rate due to stress. The inverse of the ratio of the amount of tin in the bronzes is 2.08:1.35:1.0 for JM 610:RP 3373:RP 5004 and the ratio of the initial corrosion currents is 2.54:1:39:1.0. The amount of tin in the bronze is obviously the dominant force in determining corrosion rtes of the alloys in fully aerated sea water. The massive impurity levels (4.55 wt%) in the JM 610 nail and the 4.80% zinc in RP 3373B are apparently of secondary importance in determining the initial rates. However, the long-term corrosion rates may be significantly different.

Corrosion Potentials and Site Conditions

The determination of the corrosion potential of an artefact on the seabed or in the laboratory is readily achieved with a digital voltmeter, a reference electrode (calomel or Ag/AgC1) and a platinum electrode. Some archaeologists and conservators remain reserved in their judgment as to whether the various Ecorr values mean anything. This section of the paper reports on a series of Ecorr measurements on the artefacts in sea water where the effects of oxygen levels, stirring and pH were noted (see Table III). The data collected on representative samples of the alloys examined in the preceding section showed that the corrosion potential measurement by itself is very sensitive to changes in corrosion behaviour. The results are discussed under separate headings of copper, brass and bronze.

Copper: RP 3074 and JM 160/T8

The two copper samples showed up differences in their behaviour immediately after immersion in sea water. The more 'reactive' copper spike (see Table II) had a corrosion potential that rapidly changed with time. The Ecorr of RP 3074 followed a $t^{½}$ dependence for twenty minutes with the potential being given by Ecorr = -0.144 –0.0108 $t^{½}$. The less reactive JM 160/T8 (see Table II) showed no rapid change in the same situation when the as-polished metal sections were first exposed to oxygenated sea water. No significant differences in behaviour of the two copper fittings were observed during the stirring of the solution or during deoxygenation. Stirring was effected by a magnetic follower and de-aeration was achieved with a bubbling stream of oxy-free nitrogen. The greatest fall in corrosion potential occurred in the 7-10 minutes it took to lower the dissolved oxygen level from 6.8±0.2 to zero ppm. Assuming that the corrosion potentials are in a region where there is a linear relationship between log i_{corr} and Ecorr, the 26mV fall for RP 3074 would indicate that the corrosion rate had fallen by a factor of 3 and the 40mV fall for JM610/T8 gives a five fold decrease. These calculations are based on the mean value of 56±mV for the Tafel decadic slope for oxidation of copper alloys in sea water. [29]

Brass:

The Ecorr of the RP 0000/T13 brass spike was essentially independent of the time spent sitting in sea water and didn't change with stirring. Deoxygenation of the solution caused the Ecorr to fall initially by 18mV but the Ecorr gradually drifted back to its initial value of –0.006 volts which may indicate a change-over in corrosion mechanism, i.e. instead of the copper-rich phases corroding under oxygenated conditions the zinc-rich dendrites can corrode preferentially at low oxygen potentials.

The more reactive brass sample, EG 1379/T2, showed a marked time dependence of the corrosion potential that was largely determined by the dissolved oxygen level (see fig. 5). During the initial immersion in sea water the concentration of oxygen fell from 11.8 to 6.3 ppm and the Ecorr fell by 62mV according to the equation Ecorr = -0.192 –0.021 log t, for 45 ≤ t ≥ 5 minutes. Stirring had little effect on the Ecorr. During degassing with nitrogen the Ecorr again fell logarithmically with time with Ecorr = -0.250 –0.046 log t, for 7 ≤ t ≥ 2 minutes and a total fall of 67mV (see Table III). On standing for 24 hours the dissolved oxygen level had returned to 8.3 ppm and Ecorr returned to the same value (-0.211 volts) it had during the initial immersion.

Using the decadic Tafel slope of 56mV we can calculate that the decrease in Ecorr of 18mV on deoxygenation for RP 0000/T13 corresponds to a two-fold reduction in corrosion rate while the 67mV change for EG 1374/T2 implies a fall in corrosion rate by a factor of almost sixteen.

Bronze:
The arsenical bronze nail JM 610 showed the same dependence of Ecorr on standing in sea water as the brass nail from the Eglinton with Ecorr being given by the relationship Ecorr = 0.168 –0.019 log t as the oxygen concentration fell from 5.5 ppm to 4.2 ppm. The plateau value of -0.191 was reached after 45 minutes. Stirring the solution had no effect. Ecorr fell by a further 53mV after degassing with oxy-free nitrogen for ten minutes. The same behaviour of the arsenical bronze JM 160 and the *Eglinton* brass nail is seen in not only the same response of Ecorr to oxygen (see Table III) but also in the same calculated i_{corr} values for oxygen saturated sea water since 28.3 and 29.2μA/cm^2 are well within the 13% reproducibility range of Rp data.

Addition of HC1 to the sea water changed the Ecorr and the pH of the solution in accordance with the redox equilibrium.

$$Cu_2O + 2H^+ \leftrightarrow 2Cu^{2+} + H_2O + 2e^-$$

where the voltage is given by $E_{NHE} = 0.203 + 0.0591pH + 0.0591 \log Cu^{2+}$. [30]

The Ecorr of the high leaded zinc bronze nail RP 3373B decreased on standing in sea water according to the relationship Ecorr = -0.175 –0.0098 log t until it reached a plateau value of –0.186 volts. The corrosion potential was significantly affected by stirring, with Ecorr falling to –0.221 volts after 50 minutes. Degassing the sea water saw Ecorr fall by a further 132mV after one hour, but then the voltage gradually rose to –0.324 volts after six hours at zero oxygen concentration. Such behaviour is consistent with a changeover from corrosion of the copper-rich α phase in oxygenated sea water to corrosion of the tin-rich α + δ eutectoid phase. The response of Ecorr to changes in pH on addition of HC2 to the sea water solution was the same as that observed for JM 160.

The response of the leaded bronze nail RP 5004/T11 to immersion in sea water was minimal in that the corrosion potential didn't change after standing for an hour or being stirred for half an hour. The lack of response is consistent with this bronze having a high resistance to corrosion. Degassing with nitrogen saw the potential fall to a minimum value of –0.235 after 36 minutes (see Table III) before it gradually rose, at zero ppm dissolved oxygen, to –0.213 after 15 hours. The change in Ecorr on standing under nitrogen is very similar to the high leaded zinc bronze RP 3373B.

Inspection of the data listed in Table III of the maximum change in Ecorr on deoxygenation, prior to any changeover of mechanism, indicates that the leaded zinc brass nail RP 3373B was the most sensitive to changes in corrosion rate. The calculated decrease in corrosion rate for this nail was a factor of 227 while the decrease for the nickel-bismuth-arsenical bronze JM 610 was almost 9 and the decrease for the high bronze nail RP 5004 was almost six fold.

Conclusion
Electrochemical measurements on a range of copper, brass and bronze fittings have shown that reproducible values of the corrosion currents (i_{corr}) deduced from polarisation resistance data provide an insight into the stability of artefacts. Apparently anomalous differences in i_{corr} values can be understood in terms of the microstructure and microhardness of the metals and the effect of impurities. The proportions of the major alloying elements of tine and zinc generally dominate the corrosion performance of the fastenings. This work has shown that the corrosion potential, Ecorr of the artefacts is very sensitive to changes in corrosion brought about through differences in composition, mechanical stress and oxygenation. Simple measurement of the corrosion potential of artefacts can provide the conservator with a useful guide as to which object is the most unstable and therefore the most need of urgent treatment.

Acknowledgements
We are happy to acknowledge the help of our co-worker Maria Pitrun who performed the metallographic analysis. Thanks also go to Bruce Robinson at CSIRO, Floreat, for the access to the SEM and to Terry Pile at Curtin University of Technology for use of the microhardness instruments.

References

1. P.T. Gilbert, (1982), "A review of Recent Work on Corrosion Behaviour of Copper Alloys in Sea Water", *Materials Performance*, **21**:47-53.

2. W.S. Bjorndahl and K. Nobe, (1984), "Copper Corrosion in Chloride Media: Effect of Oxygen", *Corrosion*, 40(2):82-87.

3. E.D. Mor and A.M. Beccaria, (1979), "Effects of Temperature on the Corrosion of Copper in Sea Water at Different Hydrostatic Pressures", *Werkstoffe und Korrosion*, **30**:551-558.

4. R.F. Tylecote, (1979), "The Effects of Soil Conditions on the Long-Term Corrosion of Buried Tim-Bronzes and Copper", *J. Archaeological Science*, **6**:345-368.

5. N.A. North, (1982), "Corrosion Products on Marine Iron", *Studies in Conservation*, **27**:75-83.

6. N.A. North and C. Pearson, (1978), "Washing Methods for Chloride Removal From Marine Iron Artefacts", *Studies in Conservation*, **23**:174-186.

7. N.A. North and C. Pearson, (1978), "Methods for Treating Marine Iron", *ICOM Committee For Conservation, 5th Triennial Meeting, Zagreb*, 78/23/30:1-10.

8. I.D. MacLeod, (1981), "Shipwrecks and Applied Electrochemistry", *J. Electronal. Chem.*, 118:291-303.

9. I.D. MacLeod, (1989), "The Electrochemistry and Conservation of Iron in Sea Water", *Chemistry in Australia*, **56**(17):227-229.

10. I.D. MacLeod, (1989), "Marine Corrosion on Historic Shipwrecks and its Application to Modern Materials", *Corrosion Australasia*, **14**(3):8-14.

11. R.J. Taylor and I.D. MacLeod, (1985), "Corrosion of Bronzes on Shipwrecks – a Comparison of Corrosion Rates Deduced From Shipwreck Material and From Electrochemical Methods", *Corrosion*, **41**(2):100-104.

12. G.J. Henderson, (1980), "Unfinished Voyages: Western Australian Shipwrecks 1622-1850", University of Western Australia Press, p. 182-184.

13. I.D. MacLeod and N.A. North, (1980), "350 Years of Marine Corrosion in Western Australia", *Corrosion Australasia*, 5:11-15.

14. I.D. MacLeod, (1985), "The Effects of Concretion on The Corrosion of Non-Ferrous Metals", *Corrosion Australasia*, **10**(4):10-13

15. I.D. MacLeod and M. Pitrun, (1986), "The Effects of Microstructure on Long-Term Corrosion", Symposium 11, Lead Paper, *Proceedings of Conference 26, Adelaide, November*. Australasian Corrosion Association, Vol. II.

16. I.D. MacLeod and M. Pitrun, (1986), "Metallography of Copper and its Alloys Recovered from Nineteenth Century Shipwrecks", *Archaeometry: Australasian Studies*, Ed. J. Prescott, Dept. of Physics, University of Adelaide, Australia.

17. M.J. Pryor and K.K. Giam, (1982), "The Effects of Arsenic on the Dealloying of α – Brass", *J. Electrochem. Soc*., **129**(10):2157-2164.

18. E.R. Caley, (1964), "The Heterogeneity of Ancient Metals and the Sampling Problem", in *Analysis of Ancient Metals*, Pergamon Press, London, p.1-15.

19. P.T. Gilbert, (1982).

20. W.S. Bjorndahl and K. Nobe, (1984).

21. M. Stern and A.L. Geary, (1957), "Electrochemical Polarization I – A Theoretical Analysis of the Shape of Polarization Curves", *J. Electrochem. Soc*., **104**:56-63.

22. R.J. Taylor and I.D MacLeod, (1985).

23. B.C. Syrett and D.D. MacDonald, (1979), "The Validity of Electrochemical Methods for Measuring Corrosion Rates of Coper-Nickel Alloys in Sea Water", *Corrosion*, **35**(11):505-509.

24. D. Lewis, D.O. Northwood and C.F. Pearce, (1969), "Copper Microstrain and Electrode Potential", *Corrosion Science*, **9**(10):779-787.

25. K. Oishi, T. Tsuji and Y. Watanabe, (1982), "Behaviour of Various Elements in Dezincification Layer Examined by means of X-ray Micro-Analyser (XMA)", 'Proc. Int. Symp. Corros. Copper and Copper Alloys in Buildings', JCDA, Tokyo, p.256-269.

26. S.L. Archbutt and W.E. Prytherch, (1937), "Bismuth-arsenic-antimony-nickel-oxygen", Chapter 8 from *'Effects of Impurities in Copper'*, Res. Monograph 4, British Non-Ferrous Metals Res. Assn., London, p. 96-109.

27. Idem

28. K.Oishi, T. Tsuji and Y. Watanabe, (1982).

29. R. Grauer, P.J. Moreland and G. Pini, (1982), "A Literature Review of Polarisation Resistance Constant (B) Values for the measurement of Corrosion Rate", NACE, Houston, Texas.

30. M. Pourbaix, (1974), "Atlas of Electrochemical Equilibria in Aqueous Solutions", 2nd Ed. NACE, Houston, Texas, p.386.

Table I: Composition of Ships' Fastenings, wt%

		Reg. No.	Cu	Sn	Zn	Pb	Sb	Ni	Ag	Fe	Ad	Bi
Copper:												
Rapid	- spike	3074	98.14	0.0375	0.0022	0.163	0.024	0.018	0.088	0.003	0.21	0.047
James Matthews	- nail	150/T13	98.38	0.049	0.0037	0.101	0.027	0.021	0.108	0.002	0.34	0.077
James Matthews	- spike	150/T6	98.60	0.41	0.0033	0.0097	0.022	0.050	0.078	0.002	0.42	0.128
James Matthews	- nail	160/T8	98.63	0.074	0.0025	0.109	0.009	0.047	0.104	0.002	0.29	0.255
Brass:												
Rapid	- spike	0000/T13	70.04	0.32	26.39	1.90	0.049	0.074	0.078	0.165	0.022	0.014
Eglinton	- nail	1379/T2	68.54	0.29	30.61	0.61	0.008	0.058	0.059	0.165	0.068	0.082
Bronze:												
James Matthews	- nail	610	90.74	3.60	0.044	0.55	0.135	2.32	0.235	0.039	1.39	0.84
Rapid	- nail	3373B	84.43	5.53	4.80	3.76	0.141	0.064	0.111	0.244	0.29	0.025
Rapid	- nail	5004/T11	90.3	7.46	0.024	0.81	0.545	0.086	0.151	0.086	0.042	0.231

Table II: Polarisation Resistance Values and Corrosion Currents* for Copper Alloys in Sea Water

		Reg. No.	Surface area cm^2	Rp ohm	i_{corr} $\mu A/cm^2$
Copper:					
Rapid	- spike	3074	0.788	465	29.9
James Matthews	- nail	150/T13	1.68	220	29.8
James Matthews	- spike	150/T6	2.45	550	8.1
James Matthews	- nail	160/T8	1.38	957	8.2
Brass:					
Rapid	- spike	0000/T13	1.0	675	16.2
Eglinton	- nail	1379/T2	0.33	1187	28.3
Bronze:					
James Matthews	- nail	610	0.25	1500	29.2
Rapid	- nail	3373B	0.29	2375	16
Rapid	- nail	5004/T11	0.20	4650	11.5

*Note: All corrosion currents are approximately one order of magnitude higher than typical long-term values owing to the short equilibrium times used in this experiment. [11] The dissolved oxygen level was 17.2 ppm with flowing sea water stirred by a magnetic follower and bubbling oxygen.

Table III: Corrosion Potentials of Copper, Brass and Bronze Fittings in Sea Water*

	Initial	Rest	Stirred	Deoxygenated	$\Delta O_2 - N_2{}^{\alpha}$ mV
Copper:					
RP 3074	-0.144	-0.199	-0.212	-0.238	-26
JM 160/T7	-0.188	-0.183	-0.204	-0.244	-40
Brass:					
RP 0000/T13	-0.218	-0.218	-0.226	-0.244	-18
EG 1374/T2	-0.164	-0.226	-0.235	-0.302	-67
Bronze:					
JM 610	-0.174	-0.191	-0.193	-0.246	-53
RP 3373B	-0.170	-0.186	-0.221	-0.353	-132
RP 5004/T11	-0.191	-0.191	-0.192	-0.235	-43

* Voltages are measured relative to the saturated calomel electrode (SCE) whose potential was 0.244±0.002 volts vs NHE.

α The values of $\Delta O_2 - N_2$ refer to the change in corrosion potential of the metals between equilibrium in the stirred oxygenated solution and after deoxygenation.